Dynamics of Skirting Droplets

Caleb Akers, Dr. Jacob Hale, DePauw University, Greencastle, IN 46135

Summer 2014

Introduction

Imagine a rain drop falling onto a pond. To the naked eye, it appears that the drop instantly joins the pond water, but high-speed imaging reveals the droplet sits on top of the pond for a brief, but finite time. The act of the droplet not joining the bulk fluid is referred to as non-coalescence. The accepted theory for this phenomenon is that a thin air film separates the droplet from the bulk until the film drains away. This phenomenon can be prolonged through adding surfactants to the solution[1], constantly oscillating the bath[2], or putting the droplet in relative motion with the bath[3]. This study develops a quantitative analysis of the non-coalescence phenomenon with freely-moving, slowing droplets skirting across the water. The droplet slows exponentially and the decay constant appears to increase linearly with drop size. We also show that the droplet is likely rolling on top of the surface, rather than purely skirting, and might actually be "spinning-out" on the surface.

Figure 1: A drop skirts across the bulk water before coalescing.

Methods

The surfactant solution is 2% Triton X-100, a lab-grade surfactant, mixed with a volume of deionized water. The drops fell onto a glass ski-slope that allowed for a smooth transition into the water. High-speed cameras captured a top-down view, low-angle top view, and a low-angle bottom view of the skirting droplets. Using Image J, the top-down drops could be automatically tracked, giving the position and area of the drops at every frame, which was then analyzed through Excel. The low-angle shots had to be analyzed by hand to measure the major and minor axis, as well as the cross-section of the contact area.

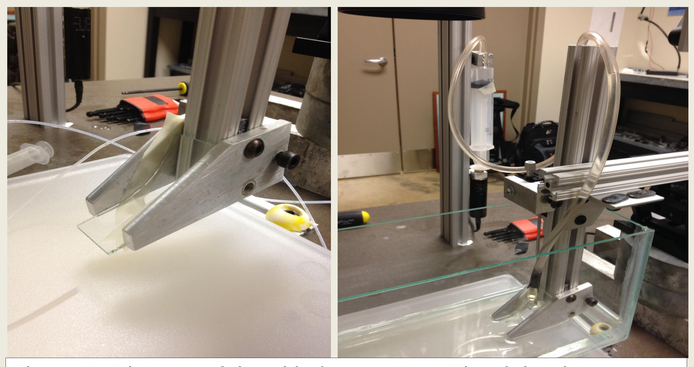

Figure 2: Pictures of the ski-slope set up. The right picture shows the syringe and motor set up that allowed for precise release of single droplets at a time.

Data and Analysis

After time and pixel cropping the videos, they were taken into Image J to acquire the data. Using built-in programs, Image J found the edges of the drop in all frames through pixel gradients and thresholded the video to remove most noise due to refraction that could affect the data. The "Analyze Particles" program then took the thresholded video and fit an ellipse mask to it and tracked the position of the mask at every frame, along with its major and minor axis and area. This analysis was truncated with area and circularity parameters to only include the best data with as little noise included as possible.

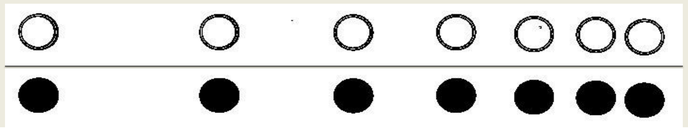

Figure 3: Above, Edges found and thresholded image of Fig. 1. Below, tracking mask of Fig 1.

Initial analysis revealed the trajectories' velocities followed an exponential decay. Fig.4 shows this decaying exponential through the average of every 20 velocity data points. Fig. 5 shows a control graph of the major and minor axis over time. When the error in the major axis dropped below a certain value, the trajectory was truncated as this was the point when the droplet came out of its plowing phase. Visually, when the major and minor axis come together, this also reveals a stable stage of the droplet.

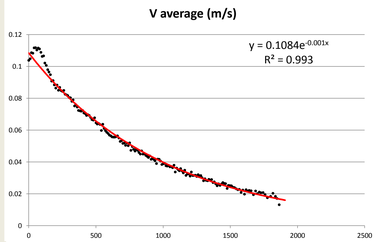

Figure 4: A standard average velocity vs time graph showing a decaying exponential.

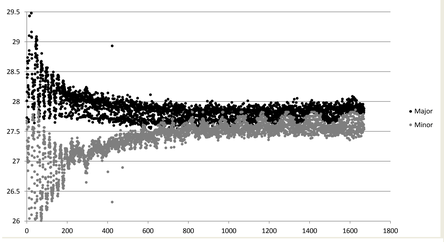

Figure 5: A graph of the major and minor axis over time used as a control to find the stable state of the droplet.

We also took side views from slightly above and slightly below the fluid surface to measure the major axis, a, minor axis, c, and the cross section of the contact area between the drop and the surface. These values were then used to find the contact area of the droplet using the equation in Fig.6 which was calculated by integrating the surface area integral from 0 to x_m.

$$A = \pi a^2 \left[1 + \frac{1}{a^2}\sqrt{(a^2 - {x_m}^2)(a^2 - \varepsilon^2 {x_m}^2)} + \left(\frac{1-\varepsilon^2}{\varepsilon}\right) ln \left|\frac{\varepsilon\sqrt{a^2 - {x_m}^2} + \sqrt{a^2 - \varepsilon^2 {x_m}^2}}{a(1-\varepsilon)}\right|\right]$$

Figure 6: Contact Area equation used for the final analysis.

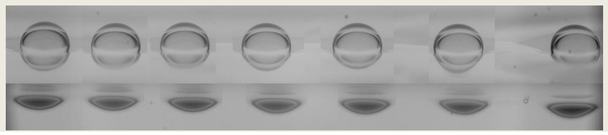

Figure 7: Above, slightly above view moving left. Below, slightly below view moving to the left.

Model Comparison and Results

Using the data, we compared averages of the decay constants of the exponential decays, τ, first to the drop sizes. This revealed a good linear fit.

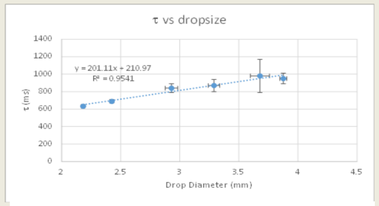

Figure 8: A linear fit of the decay constant vs the drop size reveals a strong relationship between the size and velocity decay.

Through derivation, we found a model that should explain the dynamics of the droplet.

$$v(t) = v_0 e^{-\frac{t}{\tau}}; \frac{dv}{dt} = -v_0 \frac{1}{\tau} = a$$

$$F = -\frac{\mu A v_s}{h}; F = ma$$

$$\frac{\mu A v_s}{h} = \frac{m}{\tau} v_{cm}; \frac{\mu A \alpha v_{cm}}{h} = \frac{m}{\tau} v_{cm}$$

$$\tau = \frac{\rho V h}{\mu A \alpha} \rightarrow \tau\left(\frac{\rho V}{\mu A}\right)$$

Using this relationship, the slope of our line should be the height of the air film divided by a viscosity factor, α, which we can approximate from the analysis of the bead videos. The graph of this relationship, though, shows a sigmoidal relationship, pointing to the idea that the droplets might go through a regime change as they change size. While there is background knowledge to suggest this might be true, we have not yet analyzed this possibility due to time constraints.

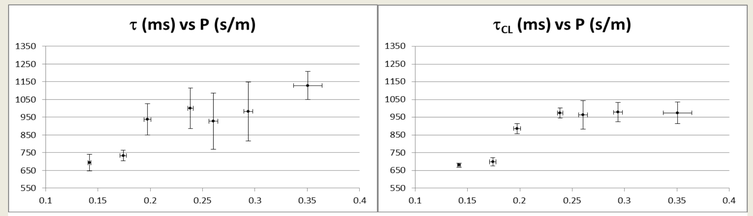

Figure 9: Average τ vs ρV/μA graph showing the sigmoidal nature.

Figure 10: Average τ vs ρV/μA graph, with a constant trajectory length of 700 ms

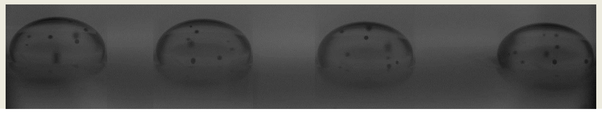

Figure 11: Droplet with beads suspended in it to monitor the internal flow.

The final part of the experiment involved suspending neutrally buoyant micro beads in the solution to model the internal flow within the droplet. After analyzing the bead videos, we saw that the tangential speeds of the beads within the droplet were nearly always greater than the translational speed of the droplet. This means the droplet is likely "spinning-out" on the fluid surface.

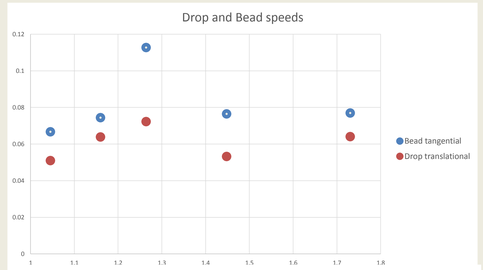

Figure 12: A graph of the average velocities of the bead (blue) and the droplet (orange) which reveals that the bead, representing the internal flow of the droplet, is moving faster than the droplet.

References:
[1] Y. Amarouchene, G. Cristobal, and H. Kellay, Phys. Rev. Lett. 87(20) (2001).
[2] H. Lhuissier, Y. Tagawa, T. Tran, C. Sun, J. Fluid Mech, (2013).
[3] I. Klyuzhin, F. Ienna, B. Roeder, A. Wexler, G. Pollack, J. Phys. Chem. B (114) (2010).